

Partial Differential Equation-Based Process Control for Ultraviolet Curing of Thick Film Resins

Adamu Yebi¹

International Center for Automotive Research,
Clemson University,
4 Research Drive,
Greenville, SC 29607
e-mail: ayebi@clemson.edu

Beshah Ayalew

Associate Professor
Mem. ASME
International Center for Automotive Research,
Clemson University,
Greenville, SC 29607
e-mail: beshah@clemson.edu

This paper proposes a feedback control system for curing thick film resins using ultraviolet (UV) radiation. A model-based distributed parameter control scheme is constructed for addressing the challenge of achieving through cure while reducing temperature gradients in thick films in composite laminates. The UV curing process is modeled with a parabolic partial differential equation (PDE) that includes an in-domain radiative input along with a nonlinear spatial attenuation function. The control problem is first cast as a distributed temperature trajectory-tracking problem where only surface temperature measurements are available. By transforming the original process model to an equivalent boundary input problem, backstepping boundary PDE control designs are applied to explicitly obtain both the controller and the observer gain kernels. Offline optimization may be used to generate the desired temperature trajectory, considering quality constraints such as prespecified spatial gradients and UV source limitations. The workings and the performance of the proposed control scheme are illustrated through simulations of the process model. It is shown that feedforward compensation can be added to achieve improved tracking with the PDE controller in the presence of measurement noise and other process disturbances. [DOI: 10.1115/1.4030818]

Keywords: UV curing process control, distributed parameter control, in-domain control of PDEs, backstepping control, curing of composite laminates

Introduction

Due to the high cost and complexity of processing advanced composite materials, their application has historically been restricted to niche sectors such as aerospace, marine, and sporting goods industries.² The cost of raw materials has been dropping in recent decades [3]. Aggressive research initiatives target to bring this cost further down to the competitive level of structural steels and alloys [4]. However, even if this aspect is overcome, the cost and complexity of processing composites remains a major barrier to their widespread use for various lightweight design applications, such as car bodies and other structures.

The prominent processes for curing composites involve the use of autoclaves and ovens. These typically feature high capital costs, high energy consumption, and long processing times (>4 hrs, for thick composite laminates), and have difficulty accommodating large size parts (e.g., airplane wings, wind turbine blades, etc.) [5,6]. Alternatives to autoclave processes are radiation-based technologies, such as microwave, infrared, electron beam, X-ray, and UV curing processes. These radiation-based processes provide the following potential advantages: (1) higher energy efficiency; (2) less environmental pollutions; (3) accelerated processing time; (4) reduced space usage; and (5) better controllability [7–11].

Among these radiation-based processes, UV curing has the advantages of low costs of the equipment, low energy consumption, and least hazardous radiation wavelengths [12]. Despite these advantages, the thickness of laminates that can be cured

effectively by UV-radiation is limited because UV gets absorbed when passing through target materials [13]. As a result, extended irradiation may be needed to cure thick sections. However, the accompanying thermal gradients from the distributed exothermic cure reactions often compromise the quality of the end product. To overcome this through-cure or cure penetration problem, an approach of layer-by-layer deposition and curing of composite laminates is often adopted. Duan et al. [5] presented such a layered manufacturing approach including experimental verifications which showed that the mechanical properties of the end product are indeed improved. Wang [14] conducted model-based investigations of in situ UV-laser curing of polymer composites using the filament winding method. By applying the UV-laser on the tow while it is being wound on the mandrel, he postulated that it might be possible to cure objects of unlimited thickness in a layered fashion.

The challenge of UV curing of thick composite laminates individually, as well as with the layered approaches, can be advanced further by incorporating proper process control that directly attempts to address the through-cure problem. This article deals with the modeling and control of single layer one-dimensional UV-curing to minimize nonuniformity of cure-level (across depth) and process energy requirements. This work could be a necessary first step toward maximizing the critical laminate thickness for each step of the layered approach, and thereby to minimize the number of layer depositions needed for manufacturing thick composite parts.

There are three challenges to process control design for this application. First, the UV curing processes involves an actuator (UV source) physically located outside the target domain that acts as a spatially distributed in-domain process input. The process input energy transferred by radiation is attenuated farther in the domain of the target because of photo-absorption [15]. This attenuation is often modeled by Beer–Lambert’s law [15]. The control design should compensate for this input attenuation.

¹Corresponding author.

²While our discussion and reviews here focus on composite laminates, the reader could see that the proposed approach can be directly applied for other thick resin film UV curing applications such as 3D printing [1,2].

Contributed by the Dynamic Systems Division of ASME for publication in the JOURNAL OF DYNAMIC SYSTEMS, MEASUREMENT, AND CONTROL. Manuscript received May 5, 2014; final manuscript received June 7, 2015; published online July 27, 2015. Assoc. Editor: YangQuan Chen.

Second, the control design needs to optimize product quality and energy requirements considering the nonlinear and distributed parameter nature of the physical processes involved: irradiation, photopolymerization, and heat transfer. These processes in UV curing lead to a nonlinear and coupled system of a PDE and an ordinary differential equation (ODE). Third, the control design needs to incorporate proper state estimation mechanisms to deal with the lack of robust and economical sensing alternatives for the distributed process state.

While there appears to be limited prior work on process control specific to UV curing applications, related thermal composite curing processes have been studied in Refs. [6,16–18]. Considering the optimality of the autoclave composite curing process, Dufour et al. [6] proposed a two-step model predictive control (MPC) scheme comprising of an offline nonlinear MPC (NMPC) and online linear MPC structure. For a similar autoclave curing problem, Parthasarathy et al. [16] proposed a control algorithm that augments an offline optimization, discrete interval online MPC, and a nonlinear controller. In another work, Pillai et al. [17] implemented a model-based open-loop optimal surface temperature generation scheme within a knowledge-based supervisory system.

Most of the controller implementations cited above assume either the prediction of the process state and/or the process output obtained from available sensor measurements. Others have directly addressed the issue of state estimation for feedback purposes. Soucy [18] uses an estimate of the degree of cure obtained via an extended Kalman filter in a gain-scheduled proportional-derivative controller for an autoclave composite curing process. The estimator construction assumed the online measurement of distributed temperature state. For a similar problem, Parthasarathy et al. [16] introduced a nonlinear observer to estimate primarily the distributed temperature state. The cure level state is subsequently computed from the estimated temperature.

In the above reviewed works, the controller and observer designs involved model reductions applied to the coupled PDE and ODE describing the process model. The first group of methods often proposed for model reduction of similar (nonlinear) PDE processes involve applying Karhunen–Loève expansion along with Galerkin’s projection and approximate inertial manifolds to extract a reduced-order model for the process [19–21]. The second group of methods involve applying direct finite difference methods to extract the reduced-order model that can be used for subsequent controller/observer design [6,16,18].

The reduced-order model-based design of controllers and observers for fundamentally distributed parameter systems (DPS) has some known deficiencies. Balas [22] argued that the combined control and observation spillover effects that arise from using the reduced model could be potentially destabilizing when the designs based on the reduced model are applied to the actual DPS process. For this and related reasons, controller and observer designs that directly use the original DPS model are gaining more attention [23,24]. Still, while a large collection of research can be found on the control of DPS described by a system of linear PDEs, far fewer address the control of DPS described by nonlinear PDE (NPDE) such as those that describe the curing process. Among the later, Vazquez and Krstic [25] designed an infinite-dimensional backstepping feedback controller for NPDE problems by transforming the NPDE to a stable linear PDE using nonlinear spatial Volterra series representations. However, the approach is limited to boundary control problems.

The problem under consideration for UV curing of thick resins does not quite fit the boundary control paradigm directly. However, there are few works that extend the boundary backstepping control design method for in-domain input problems of linear PDEs. Tsubakino et al. [26] introduced an additional transformation to accommodate in-domain scalar inputs multiplied by spatial functions within the boundary control scheme. Their transformation holds under the condition that the spatial function is a solution of a specifically parameterized ODE. Considering a linear

diffusion-dominated problem with in-domain spatial attenuation of the input, the authors of the present paper also derived an infinite-dimensional backstepping controller and observer by first developing a transformation from an in-domain control problem to an equivalent boundary control structure [27]. In this paper, this approach is extended to the system model comprising the NPDE of the UV curing process. This is achieved by deriving special transformations that embed the nonlinearity in the transformation. The controller is incorporated as a state trajectory-tracking controller. The desired trajectory of distributed temperature profile is determined by offline optimization that considers constraints imposed to achieve process optimality (e.g., minimum deviations in cure level, minimum temperature gradient, etc.).

The remainder of the paper is organized as follows: Section 2 details the problem statement including the adopted process model for UV curing of resins in thick composite laminates and the process characteristics that motivate the proposed control structure. Sections 3 and 4 detail the derivations of the PDE controller and observer designs, respectively. Section 5 provides demonstrative simulation results. Section 6 gives the conclusions of the work.

Problem Statement

Process Modeling. We consider a one-dimensional UV curing process for a fiberglass composite laminate. A schematic of the process setup is shown in Fig. 1. The basis for the model is that of a UV curing process model verified for a pure unsaturated polyester resin [28]. The following four considerations are added to the basic model. First, a resin volume fraction factor is introduced in the process model to consider the fact that only the resin portion undergoes the photopolymerization reaction [14,16]. Second, we take the average thermal properties of the resin and of the fiber for the properties of the composite laminate. Third, we model the attenuation of UV-radiation in the resin–fiber matrix in the z -direction according to Beer–Lambert’s Law, where a single attenuation constant will be taken for the laminate. This essentially assumes a uniformly wetted fiberglass and resin where the refractive indices of the fiber and resin are matched. To continue with this assumption for general cases, the attenuation constant for the combined resin–fiber matrix may need to be identified [13]. Fourth, in addition to the exothermic heat source, heat input from direct absorption of UV-radiation is modeled with an attenuated term in the domain instead of the boundary [29].

With the above four considerations, the adopted curing process model for the laminate is given by the following coupled PDE–ODE systems along with the boundary and initial conditions:

$$\left\{ \begin{array}{l} \rho c_p \frac{\partial T(z,t)}{\partial t} = k_z \frac{\partial^2 T(z,t)}{\partial z^2} + v_r \Delta H_r \rho_r \frac{d\alpha(z,t)}{dt} + \beta I_0^p \exp(-\beta z) \quad \text{on } \Omega_T \\ \frac{d\alpha(z,t)}{dt} = K(z,T) \varphi s^q I_0^p \alpha^m(z,t) (1 - \alpha(z,t))^n \quad \text{on } \Omega_T \\ K(z,T) = \exp(-E/RT_{\text{abs}}(z,t)) \exp(-\mu s p z) \quad \text{on } \Omega_T \\ k_z \frac{\partial T(0,t)}{\partial z} = h(T(0,t) - T_\infty) \quad \text{on } \Gamma_1 \\ \frac{\partial T(l,t)}{\partial z} = 0 \quad \text{on } \Gamma_2 \\ T(z,0) = T_0(z) \quad \text{on } \Omega \\ \alpha(z,0) = \alpha_0(z) \quad \text{on } \Omega \end{array} \right. \quad (1)$$

where ρ and c_p are the density and specific heat capacity of the composite laminate, respectively; k_z is the thermal conductivity of the laminate in the z -direction; $T(z,t)$ is temperature distribution at depth z and time t ; v_r is volumetric fraction of resin in the composite matrix; ρ_r is density of resin; and ΔH_r is polymerization enthalpy of resin conversion; E is activation energy; s is photo-initiator concentration; φ is pre-exponential factor of rate

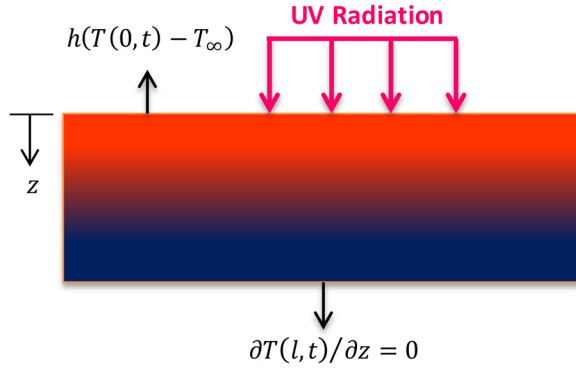


Fig. 1 Schematic for a UV curing process model

constant; R is gas constant; I_0 is UV-light intensity; $T_{\text{abs}}(z, t)$ is absolute temperature in Kelvin; $\alpha(z, t)$ is cure level distribution; m and n are reaction orders; p and q are constant exponents; μ is the absorption coefficient of photoinitiator; β is extinction coefficient of heat flux from direct UV-radiation exposure along depth; h is convective heat transfer at the top boundary; l is the thickness of composite sample, and T_∞ is constant ambient temperature; and $d\alpha(z, t)/dt$ is the rate of cure conversion (rate of polymerization). The various domains and boundaries are given by $\Omega_T \in [0, l] \times [0, \infty)$, $\Omega \in [0, l]$, $\Gamma_1 \in \{0\} \times [0, \infty)$, and $\Gamma_2 \in \{l\} \times [0, \infty)$.

For control design, we simplify the process model (1) by separating the control input and the multiplying nonlinear term, and introducing the following change of variables:

$$x = \frac{z}{l} \quad (2)$$

$$w(x, t) = T(x, t) - T_\infty \quad (3)$$

The simplified model is summarized in the following form:

$$\begin{cases} w_t(x, t) = \xi w_{xx}(x, t) + f(x, w(x, t), \alpha(x, t))u(t) & \text{on } \Omega_T \\ w_x(0, t) = \gamma_b w(0, t) & \text{on } \Gamma_1 \\ w_x(l, t) = 0 & \text{on } \Gamma_2 \\ w(x, 0) = w_0(x) & \text{on } \Omega \\ \dot{\alpha}(x, t) = \lambda_b K(x, w) \alpha^m(x, t) (1 - \alpha(x, t))^n u(t) & \text{on } \Omega_T \\ K(x, w) = \exp(-E/Rw_{\text{abs}}(x, t)) \exp(-\lambda_c x) & \text{on } \Omega_T \\ \alpha(x, 0) = \alpha_0(x) & \text{on } \Omega \end{cases} \quad (4)$$

where the nonlinear function f is defined as follows:

$$f(x, w(x, t), \alpha(x, t)) = \gamma_a K(x, w) \alpha^m(x, t) (1 - \alpha(x, t))^n + \lambda_a \exp(-\beta l x) \quad (5)$$

and $u(t) = I_0^p$ is the control input representing the incident heat flux intensity; $\xi = k_z / \rho c_p l^2$, $\gamma_a = v_r \rho_r \Delta H_r / \rho c_p$, $\lambda_a = \beta / \rho c_p$, $\lambda_b = \phi s^q$, $\lambda_c = \mu s p l$, $\gamma_b = h l / k_z$, and $w_{\text{abs}}(x, t) = w(x, t) + 273$. The notation $\dot{\alpha}$, w_t , w_x , and w_{xx} represent $d\alpha/dt$, $\partial w / \partial t$, $\partial w / \partial x$, and $\partial^2 w / \partial x^2$, respectively.

Process Characteristics. The use of UV curing in composite processing has been limited to the production and repair of relatively thin layers and parts (of thickness 2 mm or less) [30]. This is due to excessive attenuation of UV radiation as it passes through both the fiber and resin material. However, it turns out that the coupling of the UV polymerization process with thermal effects is dominant for selected resin types such as the unsaturated polyester resin considered in the current paper [31]. This coupling can be used to partially compensate for the UV attenuation by

imposing boundary conditions that promote retaining the exothermic energy of the polymerization reactions within the laminate. For polymeric materials of poor thermal conductivity, this can be achieved by insulating the boundary (or mold) at the opposite end of the UV exposure.

To illustrate the above characteristics, the process model given in Eq. (1) is simulated without control (open-loop). The corresponding cure level and temperature gradients are compared when changing the bottom boundary from constant ambient temperature to an insulated condition while keeping the top convective condition the same. For a relatively thin composite laminate of thickness 2.5 mm, with applied UV intensity of 50 mW/cm², the simulation results are shown in Figs. 2 and 3 for selected nodal points: top ($z = 0$), middle ($z = 0.5l$), and bottom ($z = l$).

The results in Fig. 2 illustrate that with the constant ambient temperature boundary condition at the bottom, there is significant cure level deviation in the laminate (maximum > 20%) with a maximum temperature deviation of only 10 °C from the ambient condition. In contrast to this, for the case in Fig. 3, there is a significant reduction of the cure level deviation (almost by 50%) by insulating the bottom boundary. This compensation is achieved because the energy loss at the bottom boundary is prevented by insulation and the temperature builds up from the bottom as the curing progresses.

To further explain how the manner the temperature builds up helps with compensating for the attenuation, we plot the cure rate factor $K(z, T)$ in the process model (1) for the bottom-insulated condition with the same UV input as above. Since the spatial input attenuation component ($\exp(-\mu s p z)$) in $K(z, T)$ is constant with time for any spatial location, the contribution of the Arrhenius component ($\exp(-E/RT_{\text{abs}}(z, t))$) is responsible for the increase in the cure rate as the temperature builds up as shown in Fig. 4. It shows that due to the coupling with the temperature evolution and the selected boundary condition, the cure rate at the bottom could be made close to that at the top for some periods of time, despite the attenuation of UV intensity with depth.

The compensation for UV attenuation via the boundary condition shown in Fig. 3 is achieved at the expense of large thermal gradients (of 15 °C) and higher operating temperatures (maximum 80 °C). To exploit the compensating benefit of such boundary conditions for relatively thicker sections (5 mm and above) where the UV attenuation may be even more significant, the temporal and spatial distributions of temperature will need to be judiciously managed in order to avoid thermal stresses that affect the quality and mechanical performance of the end product. A feedback process control scheme is proposed to achieve this objective.

Proposed Closed-Loop Control Scheme. In this paper, we devise a process control scheme that achieves a desired spatiotemporal temperature distribution during the curing process in a manner that also minimizes the cure level deviation across the layer. We propose an infinite-dimensional PDE controller that is able to track a prespecified distributed temperature trajectory. The feasible reference temperature trajectory could be generated by offline optimization considering process constraints of thermal gradient, peak temperature, cure level deviation, UV source limitations, etc.

The structure of the proposed controller is summarized in Fig. 5. Successful implementation of this closed-loop control requires that the actual temperature distribution in the laminate be available by measurement or by incorporating an observer design. Since the former is impractical, we design an infinite-dimensional (PDE) observer by assuming only the availability of measurement of the top surface temperature via an infrared thermal imaging camera.

PDE Controller Design

The PDE control design presented in this section is motivated by recent advances in infinite-dimensional control theory for boundary control problems. Since the present UV curing application is an in-domain input problem, a two-step process of PDE

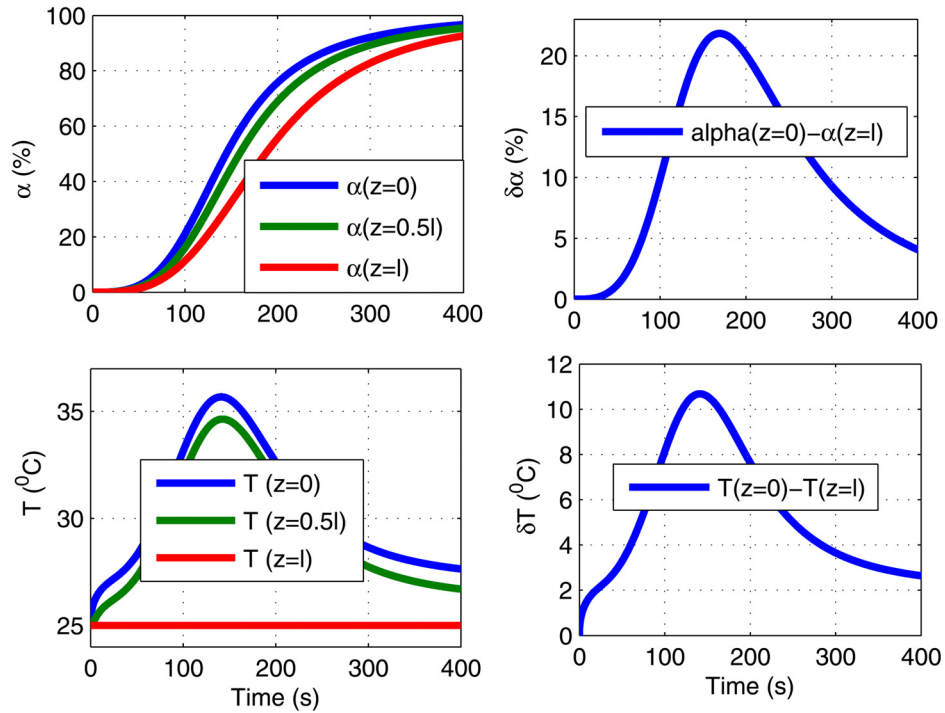


Fig. 2 Open-loop responses with constant ambient temperature boundary condition at the bottom: (a) nodal cure level distribution, (b) deviation of cure level between top and bottom, (c) nodal temperature distribution, and (d) deviation of temperature between top and bottom

controller design is proposed: (1) transforming the in-domain input problem to an equivalent boundary input problem and (2) feedback controller design for the boundary input problem. The feedback control design formulated in this section assumes availability of distributed states, and this assumption will be relaxed later via observer design.

Transforming In-Domain Input to Boundary Input. The in-domain input NPDE in Eq. (4) is transformed to an equivalent boundary input linear PDE to which standard infinite-dimensional backstepping control design methods can be applied [23]. An additional new feature here is that, through the transformation, the nonlinear term is moved to the boundary so that it can be

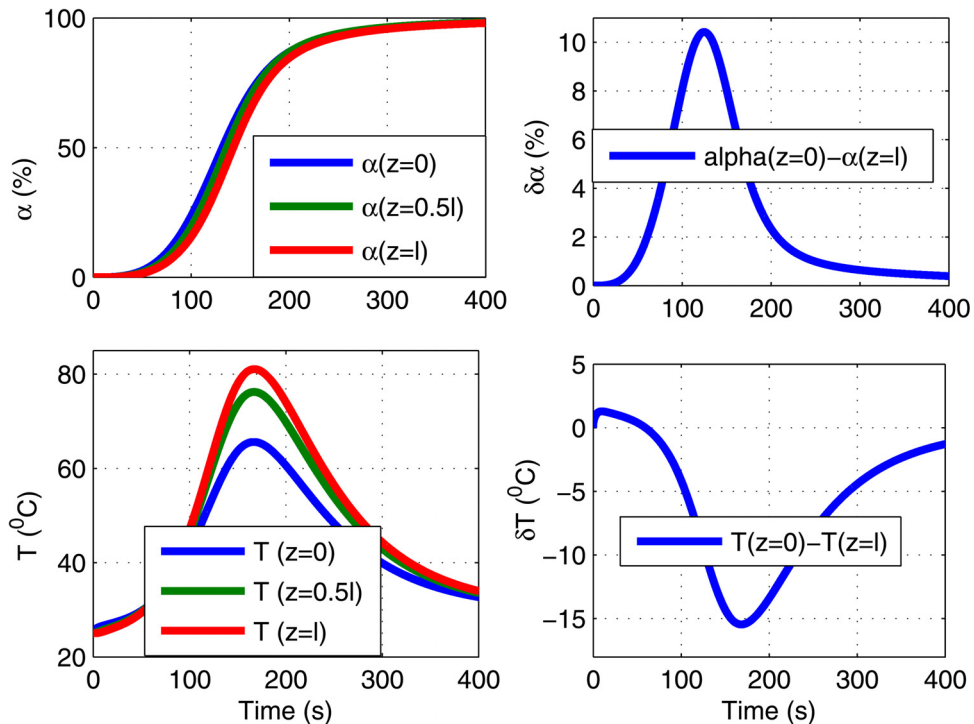


Fig. 3 Open-loop responses with insulated boundary condition at the bottom: (a) nodal cure level distribution, (b) deviation of cure level between top and bottom, (c) nodal temperature distribution, and (d) deviation of temperature between top and bottom

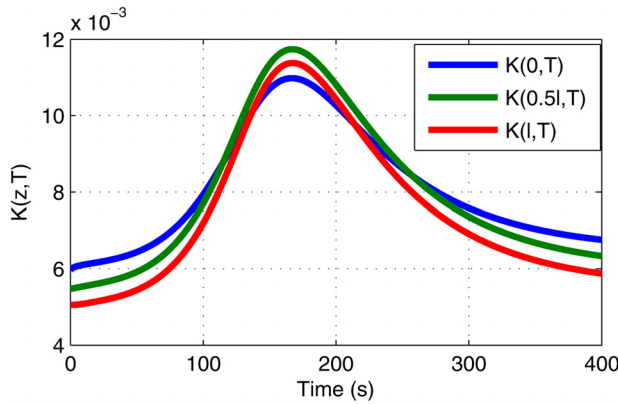


Fig. 4 The evolution of the product of spatial input attenuation and Arrhenius components with insulated boundary condition at the bottom

simultaneously handled in the boundary control design. At this point, we consider the following linear PDE as a target boundary input problem with known or desirable open-loop stability properties (in this case, a stable heat equation):

$$\begin{cases} w_t(x,t) = \xi w_{xx}(x,t) & \text{on } \Omega_T \\ w_x(0,t) = \gamma_b w(0,t) & \text{on } \Gamma_1 \\ w_x(l,t) = \bar{h}(t) & \text{on } \Gamma_2 \\ w(x,0) = w_0(x) & \text{on } \Omega \\ \dot{\alpha}(x,t) = \lambda_b K(x,w) \alpha^m(x,t) (1 - \alpha(x,t))^n u(t) & \text{on } \Omega_T \\ \alpha(x,0) = \alpha_0(x) & \text{on } \Omega \end{cases} \quad (6)$$

where $K(x,w)$ is defined in Eq. (4).

The Neumann boundary input $\bar{h}(t)$ in Eq. (6) can now be considered to include the transformation of the input along with the nonlinear term it multiplies in the original model. The main idea proposed is then finding a transformation that makes the original PDE in Eq. (4) with in-domain input to behave like a hypothetical linear PDE in Eq. (6) with this boundary input. This transformation is possible for two reasons. First, the original composite curing process which is modeled by thermal diffusion with a convective heat transfer at the boundary and a decaying polymerization rate $\dot{\alpha}(x,t)$ as the curing advances is a stable process. Second, it is possible to find a stable target system where the control objective can be achieved through secondary transformations of

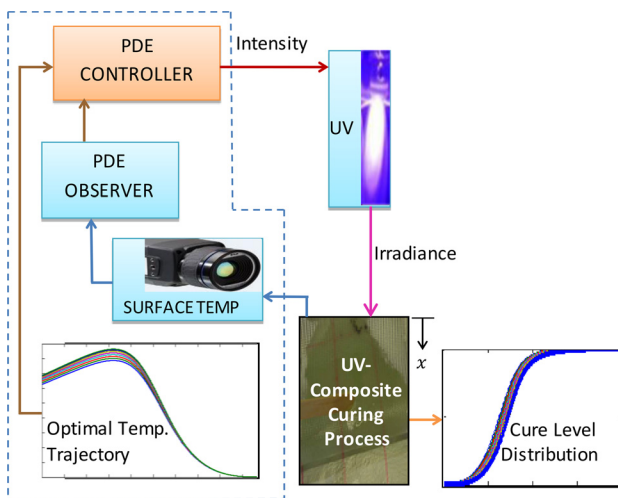


Fig. 5 Closed-loop UV curing process control system

Eq. (6) to a stable closed-loop target system. This idea is motivated by the earlier work of the authors where a linear diffusion-dominated PDE with a spatially varying in-domain input is treated [27]. A similar idea of transformation is also used in Ref. [32] for a linear PDE with in-domain point actuators as opposed to the in-domain attenuating actuation we address here.

The transformation that maps the in-domain input in Eq. (4) to the control signal $\bar{h}(t)$ appearing at the boundary in Eq. (6) can be developed by equating the weak forms of both Eqs. (4) and (6). To facilitate the weak formulations, a function space called Sobolev space is introduced as follows:

$$V: \{v \in H^1(\Omega)\} \quad (7)$$

where $H^1(\Omega) = \{v \in L^2(\Omega) | v_x \in L^2(\Omega)\}$ is the Hilbert space associated with the inner product and its norm.

Given this particular Sobolev space, the PDE (6) is multiplied with a test function $v(x) \in V$ that is chosen to be compatible with the associated boundary conditions. Then, performing integration by parts along with the boundary conditions, the weak form of the PDE in Eq. (6) is obtained

$$\begin{aligned} & \int_{\Omega} w_t(x,t)v(x)dx + \int_{\Omega} w_x(x,t) \cdot v_x(x)dx \\ &= \int_{\Gamma_2} w_x(1,t)v(x)d\sigma - \gamma_b w(0,t) \int_{\Gamma_1} v(x)d\sigma, \quad \forall w, v \in V \end{aligned} \quad (8)$$

One can prove the existence and uniqueness of the weak solution for this boundary value problem, by verifying the properties of ellipticity and continuity, following examples provided in Ref. [33].

Proceeding similarly, the following weak form of the PDE in Eq. (4) is obtained:

$$\begin{aligned} & \int_{\Omega} w_t(x,t)v(x)dx + \int_{\Omega} w_x(x,t) \cdot v_x(x)dx \\ &= \int_{\Gamma_2} g(x,t)v(x)d\sigma - \gamma_b w(0,t) \int_{\Gamma_1} v(x)d\sigma, \quad \forall w, v \in V \end{aligned} \quad (9)$$

where the intermediate in-domain input $g(x,t)$ is introduced as the product of the control signal $u(t)$ and the nonlinear term $f(x,w(\cdot,t),\alpha(x,t))$

$$g(x,t) := f(x,w(\cdot,t),\alpha(x,t))u(t) \quad (10)$$

By equating Eqs. (8) and (9), the transformation that relates the boundary input in Eq. (6) and in-domain input in Eq. (4) is given by

$$u(t) = \frac{\bar{h}(t) \int_{\Gamma_2} v(x)d\sigma}{\int_{\Omega} f(x,w(x,t),\alpha(x,t)) \cdot v(x)dx} \quad (11)$$

For solvability of this transformation, the choice of the test function should satisfy the condition

$$\int_{\Omega} f(x,w(x,t),\alpha(x,t)) \cdot v(x)dx \neq 0 \quad (12)$$

and the obliqueness of the Neumann boundary condition [34].

The test function of the form (13) is chosen as

$$v(x) = \frac{-x^2}{2} + x + \frac{1}{\gamma_b} \quad (13)$$

This test function (13) is a solution of the spatial ODE derived from the PDE and boundary conditions in Eq. (4) by neglecting

the time derivative and considering a unit in-domain input. This choice of the fundamental static solution of the PDE (spatial ODE) for a test function guarantees the solvability of the transformation map (11).

Given the test function (13) and transformation (11), a control law can be designed for the boundary control problem (6) using existing boundary control design methods, and then transform the result back to the original in-domain input problem (4).

Control Law. In this section, the control law is designed for the boundary input problem (6) using backstepping techniques described in Ref. [23]. The search for the control law starts by first defining a stable closed-loop target system. In the process of mapping the boundary input problem to the stable target system, the control law will be derived. The choice of particular stable target system is not unique, but the following exponentially stable target system is defined with tuning parameter $c > 0$:

$$\begin{cases} Z_t(x, t) = \xi Z_{xx}(x, t) - cZ(x, t) & \text{on } \Omega_T \\ Z_x(0, t) = 0 & \text{on } \Gamma_1 \\ Z_x(1, t) = 0 & \text{on } \Gamma_2 \\ Z(x, 0) = Z_0(x) & \text{on } \Omega \end{cases} \quad (14)$$

The proof for the exponential stability of a similar target system is provided in our previous work [27] and also in Ref. [35].

Then a state transformation is defined along with boundary feedback that can force the PDE in Eq. (6) to behave like the desired target system (14). The following potential state transformation is proposed in Ref. [23]:

$$Z(x, t) = w(x, t) - \int_0^x k(x, y)w(y, t)dy \quad (15)$$

By using this transformation in Eq. (14) along with Eq. (6), the following conditions can be derived for the control gain kernel:

$$k_{xx}(x, y) - k_{yy}(x, y) = \frac{c}{\xi}k(x, y) \quad (16)$$

$$k_y(x, 0) = \gamma_b k(x, 0) \quad (17)$$

$$k(x, x) = -\frac{c}{2\xi}x \quad (18)$$

The gain kernel $k(x, y)$ satisfying Eqs. (16)–(18) can be solved analytically [36]. The result is the following:

$$k(x, y) = -\frac{\bar{c}I_1\left(\sqrt{\bar{c}(x^2 - y^2)}\right)}{\sqrt{\bar{c}(x^2 - y^2)}} + \frac{\bar{c}\gamma_b}{\sqrt{\bar{c} + \gamma_b^2}} \int_0^{x-y} I_1\left(\sqrt{\bar{c}(x+y)(x-y-\tau)}\right) \exp\left(\frac{-\gamma_b\tau}{2}\right) \sinh\left(\frac{\bar{c} + \gamma_b^2}{2}\tau\right) d\tau \quad (19)$$

where $I_j(\cdot)$ is the modified Bessel function of the first kind and order j , and $\bar{c} = c/\xi$. Taking the spatial derivative of the transformation (15), and then substituting the associated boundary condition at $x = 1$, the feedback controller that completes the transformation of the PDE in Eq. (6) into target system (14) can be derived. The resulting expression for the control law is

$$\begin{aligned} \bar{h}(t) = & -\frac{\bar{c}}{2}w(1, t) + \int_0^1 \{-N_1(1, y) + N_2(1, y)\}w(y, t) \\ & + \frac{\bar{c}\gamma_b}{\sqrt{\bar{c} + \gamma_b^2}} \int_0^1 N_3(1, y)w(y, t)dy \end{aligned} \quad (20)$$

where

$$N_1(1, y) = \frac{\bar{c}I_1\left(\sqrt{\bar{c}(1 - y^2)}\right)}{\sqrt{\bar{c}(1 - y^2)}} + \frac{\bar{c}I_2\left(\sqrt{\bar{c}(1 - y^2)}\right)}{\sqrt{\bar{c}(1 - y^2)}} \quad (21)$$

$$N_2(1, y) = \frac{\bar{c}\gamma_b}{\sqrt{\bar{c} + \gamma_b^2}} \exp\left(\frac{-\gamma_b}{2}(1 - y)\right) \sinh\left(\frac{\bar{c} + \gamma_b^2}{2}(1 - y)\right) \quad (22)$$

$$N_3(1, y) = \int_0^{1-y} \frac{\bar{c}}{2}(2 - \tau) \frac{I_1\left(\sqrt{\bar{c}(1+y)(1-y-\tau)}\right) \exp\left(\frac{-\gamma_b\tau}{2}\right)}{\sqrt{\bar{c}(1+y)(1-y-\tau)}} \times \sinh\left(\frac{\bar{c} + \gamma_b^2}{2}\tau\right) d\tau \quad (23)$$

To adopt the stabilizing controller in Eq. (20) to the distributed temperature tracking problem, we define the error variable $\tilde{w}_r(x, t)$ between the actual temperature $w(x, t)$ and the reference temperature trajectory $w^r(x, t)$ as

$$\tilde{w}_r(x, t) = w(x, t) - w^r(x, t) \quad (24)$$

Here, we assume the availability of a feasible reference distributed temperature trajectory (one that satisfies the underlying PDE and boundary conditions). Substituting it into the closed-loop system involving the PDE in Eq. (6), state transformation (15), the controller (20), and exponentially stable target system (14), it can be verified that the associated error dynamics goes to zero exponentially. Following the steps outlined in Ref. [23] (p. 131), using the stabilizing controller (20) and error variable (24), the boundary control law that tracks the reference trajectory can be derived. Then, the result can be transformed back to the original in-domain control input through transformation (11). The final in-domain control signal that tracks the reference trajectory becomes

$$u(t) = \theta(t) \left\{ \frac{\bar{c}}{2}(w^r(1, t) - w(1, t)) + \int_0^1 N(1, y)(w(y, t) - w^r(y, t))dy \right\} \quad (25)$$

where

$$N(1, y) = -N_1(1, y) + N_2(1, y) + \frac{\bar{c}\gamma_b}{\sqrt{\bar{c} + \gamma_b^2}}N_3(1, y) \quad (26)$$

$$\theta(t) = \frac{\int_{\Gamma_2} v(x)d\sigma}{\int_{\Omega} f(x, w(x, t), \alpha(x, t)) \cdot v(x)dx} \quad (27)$$

and $N_1(1, y)$, $N_2(1, y)$, and $N_3(1, y)$ are as given in Eqs. (21)–(23).

PDE Observer Design

In this section, an infinite-dimensional observer is designed to estimate the distributed states for the purpose of implementing the feedback controllers. Only surface/boundary measurement of temperature is assumed available. Although the nonlinearity in the UV curing process model (4) might seem to complicate the design of the observer, the transformation of the in-domain input problem (4) to the boundary input problem (6) described above also simplifies the process of observer design. After applying the transformation (11), existing observer design methods for linear PDEs can be extended to the current problem. A number of DPS observer design methods for linear PDE are summarized in Ref. [37], including Lyapunov-based functional observers, adaptive observers, and backstepping observers. For consistency with the control design of the previous section, the backstepping technique is

adopted to design an observer for the transformed boundary input problem (6). Then, the observer so designed can be transformed back to the original in-domain input problem by using the same transformation map developed for the feedback controller.

The observer model for the transformed boundary PDE in Eq. (6) with top surface temperature measurement $w(0, t)$ is constructed in the form

$$\begin{cases} \hat{w}_t(x, t) = \xi \hat{w}_{xx}(x, t) + p_1(x)[w(0, t) - \hat{w}(0, t)] & \text{on } \Omega_T \\ \hat{w}_x(0, t) = \gamma_b w(0, t) + p_{10}[w(0, t) - \hat{w}(0, t)] & \text{on } \Gamma_1 \\ \hat{w}_x(1, t) = \bar{h}(t) & \text{on } \Gamma_2 \\ \hat{w}(x, 0) = \hat{w}_0(x) & \text{on } \Omega \\ \dot{\alpha}(x, t) = \lambda_b K(x, \hat{w}) \alpha^m(x, t) (1 - \alpha(x, t))^n u(t) & \text{on } \Omega_T \\ \alpha(x, 0) = \alpha_0(x) & \text{on } \Omega \end{cases} \quad (28)$$

where $\hat{w}(x, t)$ is the estimated state, $p_1(x)$ and p_{10} are the observer gains. Note that after estimating the temperature state $w(x, t)$, the cure state $\alpha(x, t)$ can be subsequently computed from the cure dynamics (as an open-loop observer, as we do in this paper) or by designing another cure state observer, a topic we address in Ref. [38].

Defining the estimation error variable as $\tilde{w}(x, t) = w(x, t) - \hat{w}(x, t)$ and subtracting Eq. (28) from Eq. (6), the temperature observation error system becomes

$$\begin{cases} \tilde{w}_t(x, t) = \xi \tilde{w}_{xx}(x, t) - p_1(x) \tilde{w}(0, t) & \text{on } \Omega_T \\ \tilde{w}_x(0, t) = -p_{10}(x) \tilde{w}(0, t) & \text{on } \Gamma_1 \\ \tilde{w}_x(1, t) = 0 & \text{on } \Gamma_2 \\ \tilde{w}(x, 0) = \tilde{w}_0(x) & \text{on } \Omega \end{cases} \quad (29)$$

Considering transformation of Eq. (29) to the same stable target system (14), the observer can be designed such that the origin of the error system (29) is exponentially stable. We replace the parameter c in Eq. (14) by η to distinguish between the target systems for the observer and controller designs and follow the same steps as in the control law derivation to obtain the conditions for the observer gain kernel $p(x, y)$. It turns out that the conditions on the gain kernel can be solved explicitly to derive the following observer gains:

$$p_1(x) = \eta \left(\frac{I_1(\sqrt{\eta}x(2-x))}{\sqrt{\eta}x(2-x)} + \frac{I_2(\sqrt{\eta}x(2-x))}{x(2-x)} \right) \quad (30)$$

$$p_{10} = -\frac{\bar{\eta}}{2} \quad (31)$$

where $\bar{\eta} = \eta/\xi$.

Finally, transforming the observer (28) designed for the boundary input problem (6) back to the original in-domain input PDE in Eq. (4) through transformation (11), the structure of the observer for the in-domain input PDE takes the form

$$\begin{cases} \hat{w}_t(x, t) = \xi \hat{w}_{xx}(x, t) + p_1(x)[w(0, t) - \hat{w}(0, t)] \\ \quad + f(x, \hat{w}(x, t), \alpha(x, t))u(t) & \text{on } \Omega_T \\ \hat{w}_x(0, t) = \gamma_b w(0, t) + p_{10}[w(0, t) - \hat{w}(0, t)] & \text{on } \Gamma_1 \\ \hat{w}_x(1, t) = 0 & \text{on } \Gamma_2 \\ \hat{w}(x, 0) = \hat{w}_0(x) & \text{on } \Omega \\ \dot{\alpha}(x, t) = \lambda_b K(x, \hat{w}) \alpha^m(x, t) (1 - \alpha(x, t))^n u(t) & \text{on } \Omega_T \\ \alpha(x, 0) = \alpha_0(x) & \text{on } \Omega \end{cases} \quad (32)$$

For implementation with the controller, the observer PDE in Eq. (32) can be solved using forward-in-time central-in-space (FTCS) finite difference methods. Then, using the estimated temperature state, the tracking control signal in Eq. (25) can be computed by numerical integration. In this work, first trapezoidal integration is applied with variable integration limits to reduce the double integration (also including the N functions) to a single integration. Then, Simpson's composite one-third rule is applied [39].

Results and Discussion

In this section, simulation results are presented to demonstrate the performance of the proposed PDE controller for tracking a reference distributed temperature trajectory. The associated thermal, chemical, and material constants for the process model (4) are extracted from published work [14,28]. A thickness of 5 mm is considered for the composite laminate.

Nominal Performance of the Feedback Control Scheme. We first note that while the control law derivations allow for any feasible distributed temperature trajectory (one that satisfies the underlying PDE and boundary conditions) to be tracked by the proposed controller, the design of the PDE control law itself does not consider optimality. Therefore, in this work, we generated an optimal temperature trajectory using an offline NMPC procedure [6] which explicitly targets minimizing the spatial cure deviation and the required energy input. Hard constraints are also included to limit the spatial temperature gradient and rapid heating of the laminate. One can also consider such a desired trajectory to be available from operating experience with the process.

To test the performance of the proposed PDE controller in tracking the offline generated trajectory, a coarse grid of 11 nodes and a fine grid of 26 nodes are considered for numerical FTCS implementations of the observer and process models, respectively. Also, initial conditions for the observer PDE are set/guessed to be different from that of the process. Figure 6 shows the temperature tracking performance for the bottom node and the corresponding control signal. The figure also shows how the tracking performance of the proposed controller can be tuned via the free controller design parameter c . By tuning c from 20 to 35, the controller is able to track the desired trajectory very closely, albeit at the cost of more overall control effort as shown in Fig. 6(b).

The feedback control input shown in Fig. 6(b) (that achieves near perfect tracking with $c = 35$) corresponds to the reference temperature profile that is generated offline considering optimality and constraints as mentioned above. The input is saturated here at

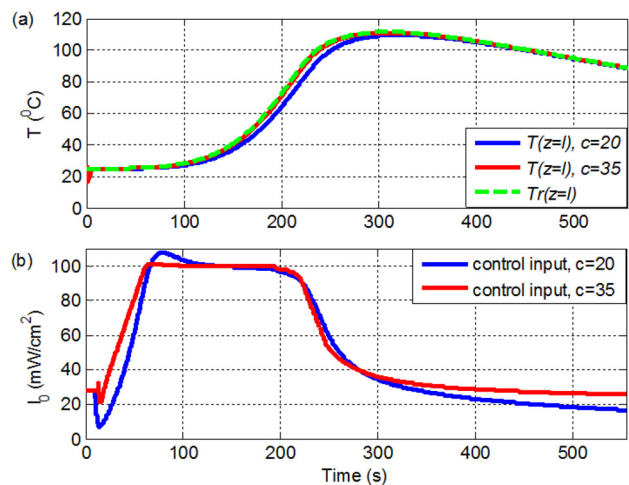


Fig. 6 (a) Temperature profile of the process at node ($z=l$) (solid line represents actual response with the proposed controller and dashed line is the reference temperature) and (b) control input

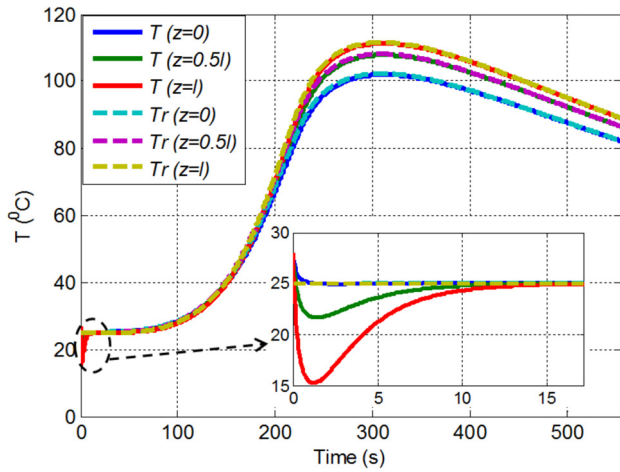


Fig. 7 Nodal temperature distribution of the process (solid line represents actual response with the proposed controller and dashed line is the reference temperature)

28.1 mW/cm² for the first few seconds to overcome overshoots associated with initial observer state guesses. Then, the control input increases until it reaches a maximum and eventually starts to decrease toward a lower steady value as the contribution of the thermal coupling becomes significant. If a different reference temperature profile is selected, the nature of the control input will also change.

Figure 7 shows the tracking performance of the proposed controller with $c = 35$ for the distributed temperature state by considering more nodal points: top ($z = 0$), middle ($z = 0.5l$), and bottom ($z = l$). It can be seen that near perfect tracking of the reference trajectory is achieved within a few seconds. This is achieved despite the inherent temperature gradient that develops as the curing progresses. The temperature at the center is closer to that of the bottom boundary because of the dominance of the convective heat transfer at the top over the conductive transfer in the domain of the laminate.

Next, we take a closer look at the cumulative gain kernel (26) in the backstepping PDE controller (25), which was designed by first transforming the in-domain input problem to an equivalent bottom boundary input problem. The computed gain kernel weighs the contribution of the tracking error at each spatial node differently to generate the required feedback control effort. Specifically, it can be seen in Fig. 8 that the gain kernel generally increases in magnitude from the bottom ($y = 1$) to the top ($y = 0$). This means the PDE controller weighs temperature-tracking errors near the top more, which is desirable given the energy retaining effect of the insulated boundary conditions at the bottom as

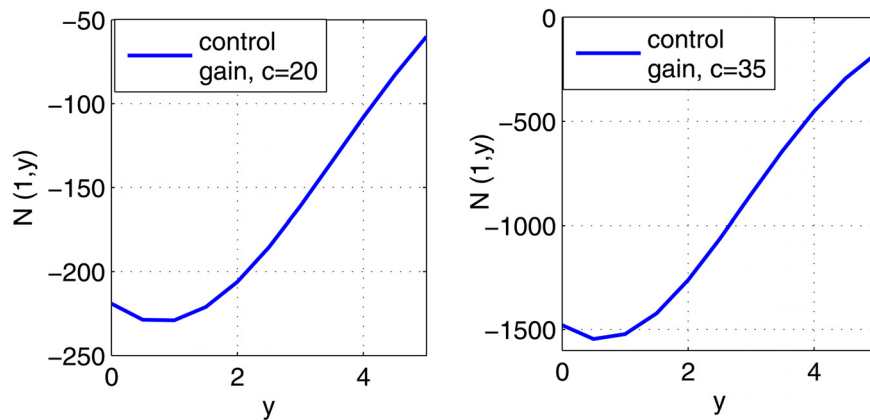


Fig. 8 Control gain kernel $N(1, y)$ for different values of c

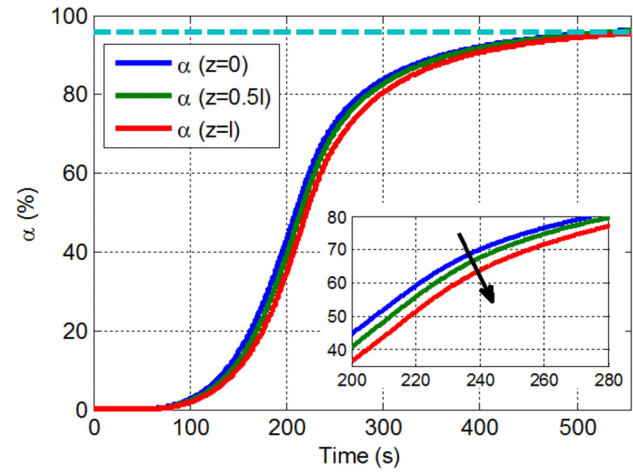


Fig. 9 Nodal controlled cure level distribution via the proposed controller

discussed in Sec. 2.2. It can also be seen in Fig. 8 that the gain kernel takes higher overall magnitudes for larger values of tuning parameter c .

By closely tracking the offline generated optimal temperature profiles, it can be seen in Fig. 9 that the proposed PDE controller achieves very low cure deviation along depth (of less than 8%) while curing to near complete cure (96%). This is achieved with a maximum in process temperature gradient of 10°C (Fig. 7).

Next, the performance of the observer is illustrated in Fig. 10, which shows the spatial distribution and the evolution of the spatial 2-norm of the observation error plotted on a faster time scale. The decay rate of the observer error can be controlled with the free design parameter η in the observer. Here, the initial temperature state error is tuned to stabilize quickly in about 15 s.

Finally, a comment is in order regarding the computational burden of the proposed approach for real-time implementation. The infinite-dimensional observer (PDE system) and controller can be approximated with the (FTCS) finite difference approximation and (trapezoidal, Simpson [39]) numerical integration similar to what we adopted for the simulation results above. The maximum sampling/discretization time needed for numerical stability is 0.54 s (for the nodal spatial discretization of the observer PDE) as can be estimated from the well-known condition for diffusion PDE's: ($\xi dt/dx^2 \leq 0.5$) [40]. Given this constraint, we evaluated the computation time needed for the MATLAB implementation of our proposed control scheme for closed-loop simulations on a modern laptop personal computer (with a Windows 8 operating system running multiple applications). For a selected sampling time of 0.05 s, the observer and controller computations always finish in much less

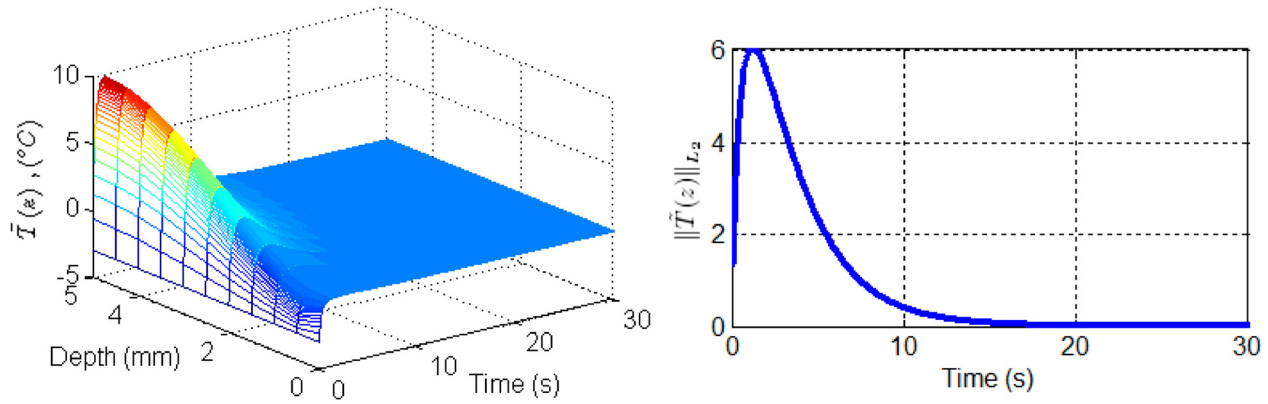


Fig. 10 Convergence of observer error (a) spatial distribution and (b) spatial 2-norm

than 0.01 s. Therefore, on a dedicated modern or future control hardware and real-time operating system, we expect that the proposed approach is quite feasible for real-time implementation.

Modified Implementation: Feedforward + Feedback. As shown above, the nominal performance of proposed feedback controller can indeed be improved by tuning the controller and observer with free parameters c and η . However, in practice, with the presence of noise in the surface temperature measurement, the control signal computed with high-gain settings is corrupted by the noise. For such practical considerations, the control structure can be modified from the pure feedback form to a combined feedback plus feedforward form. The feedforward control input can be determined in the process of optimal reference temperature generation with suitable model-based offline optimization schemes (e.g., see Ref. [6] for such a scheme in an autoclave curing

application). This feedforward control input would represent the average control input and the feedback PDE controller can be redesigned to overcome the steady-state error in the presence of noise, parameter variations, and related disturbances.

The performance of the augmented feedback plus feedforward controller is tested in the presence of measurement noise and process parameters that differ from the assumptions in the control design. A zero mean Gaussian noise with covariance $\sqrt{2}$ is added on the measured surface temperature. The process parameters are altered as follows: activation energy E reduced by 10%, and reaction orders m and n changed from 0.7 and 1.3 to 0.85 and 1.15, respectively. The process parameters are changed abruptly at time = 174 s. The simulation results for the same nodal points considered above are plotted in Fig. 11. The augmented control signal along with the feedforward component is plotted in Fig. 12.

It can be seen from Fig. 11 that the feedforward control input alone is not tracking the desired temperature trajectory well in the presence of process disturbances. However, with the added feedback term, the augmented control is able to track the desired trajectory closely despite the disturbances. From Fig. 12, it can be seen that the augmented input signal of feedback plus feedforward is closer to that of the offline optimized feedforward input before the parametric disturbances are introduced, at which point the augmented input changes as the feedback component responds to the disturbances.

We note that in the presence of measurement noise, the calculated input signal could still be quite noisy (including propagated computational noise) and may need to be filtered to match the practical bandwidth of the UV source/actuator (including its low level control electronics). In the above results, augmented control is filtered with a first-order low pass filter with a bandwidth of

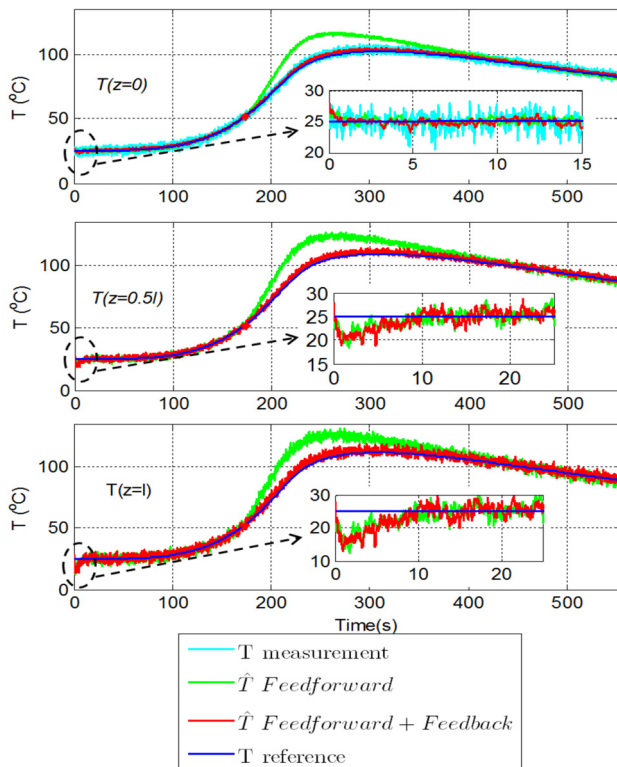


Fig. 11 Nodal temperature distribution of the process with feedforward, and feedback plus feedforward control in the presence of measurement noise

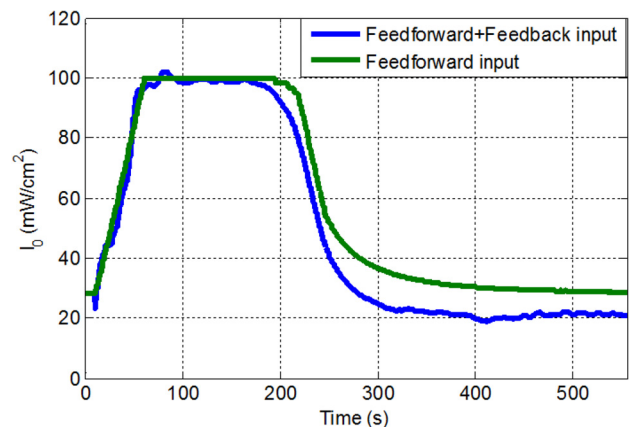


Fig. 12 Control input: feedforward and feedforward plus feedback (filtered)

10 Hz before it is applied to the process model. This filter could be considered to model the UV source dynamics, which has been ignored during the controller development.

Conclusion

This paper proposed a PDE-based process control system for radiative UV curing of thick film resins considering the in-domain attenuation of UV with depth. First, the coupling of the cure conversion with the thermal dynamics is illustrated considering the effect of choices in the temperature boundary conditions at the opposite end from the UV exposure. Then, a distributed parameter (PDE) controller is constructed to track a desired distributed temperature profile with the goal of exploiting the thermal coupling to compensate for the UV attenuation. The PDE controller is designed by transforming the original in-domain input NPDE to an equivalent boundary input linear PDE. This was realized by developing a transformation map from weak formulations of the relevant PDEs. Then, backstepping boundary control and observer designs are derived and transformed back to the original system via the identified transformation.

The performance of proposed PDE control framework was tested through simulations of the UV curing process for a 5-mm-thick laminate. The results showed that the proposed PDE controller is able to closely track the offline generated reference temperature distribution. Since the PDE controller itself is not an optimal one, the reference distribution can be generated offline considering optimality, i.e., minimization of cure level deviation across the laminate while maintaining minimal temperature gradients. In the presence of measurement noise and parametric disturbances, it was suggested that the proposed PDE feedback controller be augmented with an offline generated feedforward part to allow use of high-gain feedback for good tracking, with reduced susceptibility of the computed control signal to propagated noise.

Finally, the authors remark that other investigations could be pursued to exploit the transformations derived in this paper. In particular, after transforming similar in-domain input problems to the boundary input problem, other boundary control designs, such as the boundary predictive control design described in Ref. [41] could be tested and compared with the backstepping approach.

References

- [1] Wenbin, H., Tsui, L. Y., and Haiqing, G., 2005, "A Study of the Staircase Effect Induced by Material Shrinkage in Rapid Prototyping," *Rapid Prototyping J.*, **11**(2), pp. 82–89.
- [2] Cunico, M. W. M., and de Carvalho, J., 2013, "Optimization of Thick Layers Photopolymerization Systems Applying Experimental and Analytical Approach," *Rapid Prototyping J.*, **19**(5), pp. 337–343.
- [3] Lucintel, 2014, "Growth Opportunities in Carbon Fiber Market 2010–2015," http://www.lucintel.com/carbon_fiber_market.aspx
- [4] U.S. Department of Energy, 2011, "FY 2011 Vehicle Technologies Program, Funding Opportunity Number: DE-FOA-0000239," http://www.cooley.com/files/announce_cleantech/20101230-VTP-FOA-FY11.pdf
- [5] Duan, Y., Li, J., Zhong, W., Maguire, R. G., Zhao, G., Xie, H., Li, D., and Lu, B., 2012, "Effects of Compaction and UV Exposure on Performance of Acrylate/Glass-Fiber Composites Cured Layer by Layer," *J. Appl. Polym. Sci.*, **123**(6), pp. 3799–3805.
- [6] Dufour, P., Michaud, D. J., Touré, Y., and Dhurjati, P. S., 2004, "A Partial Differential Equation Model Predictive Control Strategy: Application to Autoclave Composite Processing," *Comput. Chem. Eng.*, **28**(4), pp. 545–556.
- [7] Thostenson, E. T., and Chou, T.-W., 2001, "Microwave and Conventional Curing of Thick-Section Thermoset Composite Laminates: Experiment and Simulation," *Polym. Compos.*, **22**(2), pp. 197–212.
- [8] Kumar, P. K., Raghavendra, N. V., and Sridhara, B. K., 2011, "Development of Infrared Radiation Curing for Fiber Reinforced Polymer Composites: An Experimental Investigation," *Indian J. Eng. Mater. Sci.*, **18**(1), pp. 24–30.
- [9] Beziers, D., Capdepu, B., and Chataignier, E., 1990, "Electron Beam Curing of Composites," *Developments in the Science and Technology of Composite Materials*, Springer, The Netherlands, pp. 73–78.
- [10] Berejka, A. J., Cleland, M. R., Galloway, R. A., and Gregoire, O., 2005, "X-Ray Curing of Composite Materials," *Nucl. Instrum. Methods Phys. Res., Sect. B*, **241**(1), pp. 847–849.

- [11] Compston, P., Schiemer, J., and Cvetanovska, A., 2008, "Mechanical Properties and Styrene Emission Levels of a UV-Cured Glass-Fibre/Vinylester Composite," *Compos. Struct.*, **86**(1), pp. 22–26.
- [12] Drobny, J. G., 2010, *Radiation Technology for Polymers*, CRC Press, New York.
- [13] Endruweit, A., Ruijter, W., Johnson, M. S., and Long, A. C., 2008, "Transmission of Ultraviolet Light Through Reinforcement Fabrics and Its Effect on Ultraviolet Curing of Composite Laminates," *Polym. Compos.*, **29**(7), pp. 818–829.
- [14] Wang, X., 2001, "Modeling of In-Situ Laser Curing of Thermoset-Matrix Composites in Filament Winding," Ph.D. dissertation, University of Nebraska, Lincoln, NE.
- [15] Perry, M. F., and Young, G. W., 2005, "A Mathematical Model for Photopolymerization From a Stationary Laser Light Source," *Macromol. Theory Simul.*, **14**(1), pp. 26–39.
- [16] Parthasarathy, S., Mantell, S. C., and Stelson, K. A., 2004, "Estimation, Control and Optimization of Curing in Thick-Sectioned Composite Parts," *ASME J. Dyn. Syst. Meas. Control*, **126**(4), pp. 824–833.
- [17] Pillai, V. K., Beris, A. N., and Dhurjati, P. S., 1994, "Implementation of Model-Based Optimal Temperature Profiles for Autoclave Curing of Composites Using a Knowledge-Based System," *Ind. Eng. Chem. Res.*, **33**(10), pp. 2443–2452.
- [18] Soucy, K. A., 1991, "Process Modeling, State Estimation, and Feedback Control of Polymer Composite Processing," Ph.D. dissertation, Washington University, Seattle, WA.
- [19] Christofides, P. D., and Daoutidis, P., 1997, "Finite-Dimensional Control of Parabolic PDE Systems Using Approximate Inertial Manifolds," *J. Math. Anal. Appl.*, **216**(2), pp. 398–420.
- [20] Baker, J., and Christofides, P. D., 2000, "Finite-Dimensional Approximation and Control of Non-Linear Parabolic PDE Systems," *Int. J. Control*, **73**(5), pp. 439–456.
- [21] Varshney, A., Pitschaiah, S., and Armaou, A., 2009, "Feedback Control of Dissipative PDE Systems Using Adaptive Model Reduction," *AIChE J.*, **55**(4), pp. 906–918.
- [22] Balas, M. J., 1979, "Feedback Control of Linear Diffusion Processes," *Int. J. Control*, **29**(3), pp. 523–534.
- [23] Krstic, M., and Smyshlyayev, A., 2008, *Boundary Control of PDEs: A Course on Backstepping Designs*, Society for Industrial Mathematics, Philadelphia.
- [24] Curtain, R. F., and Zwart, H. J., 1995, *An Introduction to Infinite-Dimensional Linear Systems Theory*, Springer-Verlag, New York.
- [25] Vazquez, R., and Krstic, M., 2008, "Control of 1-D Parabolic PDEs With Volterra Nonlinearities, Part I: Design," *Automatica*, **44**(11), pp. 2778–2790.
- [26] Tsubakino, D., Krstic, M., and Hara, S., 2012, "Backstepping Control for Parabolic PDEs With In-Domain Actuation," American Control Conference (ACC), pp. 2226–2231.
- [27] Yebi, A., and Ayalew, B., 2013, "Feedback Compensation of the In-Domain Attenuation of Inputs in Diffusion Processes," American Control Conference (ACC), pp. 2092–2097.
- [28] Matias, J. M., Bartolo, P. J., and Pontes, A. V., 2009, "Modeling and Simulation of Photofabrication Processes Using Unsaturated Polyester Resins," *J. Appl. Polym. Sci.*, **114**(6), pp. 3673–3685.
- [29] Hong, W., Lee, Y. T., and Gong, H., 2004, "Thermal Analysis of Layer Formation in a Stepless Rapid Prototyping Process," *Appl. Therm. Eng.*, **24**(2), pp. 255–268.
- [30] Shi, W., and Rånby, B., 1994, "UV Curing of Composites Based on Modified Unsaturated Polyester," *J. Appl. Polym. Sci.*, **51**(6), pp. 1129–1139.
- [31] Schwalm, R., 2006, *UV Coatings: Basics, Recent Developments and New Applications*, Elsevier, Amsterdam.
- [32] Badkoubeh, A., and Zhu, G., 2011, "Tracking Control of a Linear Parabolic PDE With In-Domain Point Actuators," *World Acad. Sci. Eng. Technol.*, **59**(6), pp. 574–579.
- [33] Knabner, P., and Angerman, L., 2003, *Numerical Methods for Elliptic and Parabolic Partial Differential Equations*, Springer Verlag, New York.
- [34] Soga, H., 1974, "Boundary Value Problems With Oblique Derivative," *Publ. Res. Inst. Math. Sci.*, **10**(3), pp. 619–668.
- [35] Smyshlyayev, A., and Krstic, M., 2010, *Adaptive Control of Parabolic PDEs*, Princeton University Press, Princeton, NJ.
- [36] Smyshlyayev, A. S., 2006, "Explicit and Parameter-Adaptive Boundary Control Laws for Parabolic Partial Differential Equations," Ph.D. thesis, University of California, San Diego, CA.
- [37] Hidayat, Z., Babuska, R., De Schutter, B., and Nunez, A., 2011, "Observers for Linear Distributed-Parameter Systems: A Survey," 2011 IEEE International Symposium on Robotic and Sensors Environments (ROSE), Montreal, Canada, Sept. 17–18, pp. 166–171.
- [38] Yebi, A., Ayalew, B., and Dey, S., 2014, "Observer Design for State Estimation for UV Curing Process," *ASME Paper No. DSCC2014-6024*.
- [39] Dehghan, M., 2001, "An Inverse Problem of Finding a Source Parameter in a Semilinear Parabolic Equation," *Appl. Math. Model.*, **25**(9), pp. 743–754.
- [40] Recktenwald, G. W., 2004, "Finite-Difference Approximations to the Heat Equation," Mechanical Engineering Department of Portland State University, Portland, OR, Class Notes.
- [41] Dubljevic, S., and Christofides, P. D., 2006, "Predictive Control of Parabolic PDEs With Boundary Control Actuation," *Chem. Eng. Sci.*, **61**(18), pp. 6239–6248.